

Aberystwyth University

The histone acetyltransferase GCN5 and the transcriptional coactivator ADA2b affect leaf development and trichome morphogenesis in Arabidopsis

Kotak, Jenna; Saisana, Marina; Gegas, Vasilis ; Pechlivani, Nikoletta ; Kaldis, Anthanasios; Papoutsoglou, Panagiotis; Makris, Athanasios; Burns, Julia; Kendig, Ashley L.; Sheikh, Minna; Kuschner, Cyrus E.; Whitney, Gabrielle; Caiola, Hanna; Doonan, John; Vlachonasios, Konstantinos; McCain, Elizabeth R.; Hark, Amy T.

Published in:

Planta

DOI:

[10.1007/s00425-018-2923-9](https://doi.org/10.1007/s00425-018-2923-9)

Publication date:

2018

Citation for published version (APA):

Kotak, J., Saisana, M., Gegas, V., Pechlivani, N., Kaldis, A., Papoutsoglou, P., Makris, A., Burns, J., Kendig, A. L., Sheikh, M., Kuschner, C. E., Whitney, G., Caiola, H., Doonan, J., Vlachonasios, K., McCain, E. R., & Hark, A. T. (2018). The histone acetyltransferase GCN5 and the transcriptional coactivator ADA2b affect leaf development and trichome morphogenesis in Arabidopsis. *Planta*, 248(3), 613-628.
<https://doi.org/10.1007/s00425-018-2923-9>

General rights

Copyright and moral rights for the publications made accessible in the Aberystwyth Research Portal (the Institutional Repository) are retained by the authors and/or other copyright owners and it is a condition of accessing publications that users recognise and abide by the legal requirements associated with these rights.

- Users may download and print one copy of any publication from the Aberystwyth Research Portal for the purpose of private study or research.
- You may not further distribute the material or use it for any profit-making activity or commercial gain
- You may freely distribute the URL identifying the publication in the Aberystwyth Research Portal

Take down policy

If you believe that this document breaches copyright please contact us providing details, and we will remove access to the work immediately and investigate your claim.

tel: +44 1970 62 2400

email: is@aber.ac.uk

[Click here to view linked References](#)

The Histone Acetyltransferase GCN5 and the Transcriptional Coactivator ADA2b Affect Leaf Development and Trichome Morphogenesis in *Arabidopsis*

Jenna Kotak^{1#}, Marina Saisana², Vasilis Gegas^{3^}, Nikoletta Pechlivani², Athanasios Kaldis², Panagiotis Papoutsoglou², Athanasios Makris², Julia Burns¹, Ashley L. Kendig¹, Minnah Sheikh¹, Cyrus E. Kuschner¹, Gabrielle Whitney¹, Hanna Caiola¹, John H. Doonan³, Konstantinos E. Vlachonasios^{2*}, Elizabeth R. McCain¹, and Amy T. Hark^{1*}

¹ Biology Department, Muhlenberg College, Allentown, PA, USA

² Department of Botany, School of Biology, Aristotle University of Thessaloniki, Thessaloniki, Greece

³ National Plant Phenomics Centre, Aberystwyth University, Aberystwyth, UK

[#] Current address: Molecular Biology, Cell Biology, and Biochemistry Department, Brown University, Providence, RI, USA

[^] Current address: Limagrain UK Ltd, Joseph Nickerson Research Centre, Rothwell – Market Rasen, Lincolnshire, UK

* Corresponding authors: Amy Hark, amyhark@muhlenberg.edu, +1-484-664-3747 (phone), +1-484-664-3002 (fax); Konstantinos Vlachonasios, kvlachon@bio.auth.gr, +30-2310998833 (phone), +302310998389 (fax)

Main conclusion:

The histone acetyltransferase GCN5 and associated transcriptional coactivator ADA2b are required to couple endoreduplication and trichome branching. Mutation of *ADA2b* also disrupts the relationship between ploidy and leaf cell size.

Keywords: endoreduplication, epigenetics, chromatin, histone acetyltransferase

ABSTRACT

Dynamic chromatin structure has been established as a general mechanism by which gene function is temporally and spatially regulated, but specific chromatin modifier function is less well understood. To address this question, we have investigated the role of the histone acetyltransferase GCN5 and the associated coactivator ADA2b in developmental events in *Arabidopsis thaliana*. *Arabidopsis* plants with T-DNA insertions in *GCN5* (also known as *HAG1*) or *ADA2b* (also known as *PROPORZI*) display pleiotropic phenotypes including dwarfism and floral defects affecting fertility. We undertook a detailed characterization of *gcn5* and *ada2b* phenotypic effects in rosette leaves and trichomes to establish a role for epigenetic control in these developmental processes. ADA2b and GCN5 play specific roles in leaf tissue, affecting cell growth and division in rosette leaves often in complex and even opposite directions. Leaves of *gcn5* plants display overall reduced ploidy levels,

1
2
3
4
5 while *ada2b-1* leaves show increased ploidy. Endoreduplication leading to increased
6 ploidy is also known to contribute to normal trichome morphogenesis. We demonstrate
7 that *gcn5* and *ada2b* mutants display alterations in the number and patterning of trichome
8 branches, with *ada2b-1* and *gcn5-1* trichomes being significantly less branched while
9 *gcn5-6* trichomes show increased branching. Elongation of the trichome stalk and
10 branches also vary in different mutant backgrounds, with stalk length having an inverse
11 relationship with branch number. Taken together, our data indicate that in *Arabidopsis*
12 leaves and trichomes ADA2b and GCN5 are required to couple nuclear content with cell
13 growth and morphogenesis.
14
15
16
17
18
19
20
21
22
23
24
25
26
27
28
29
30
31
32
33
34
35
36
37
38
39
40
41
42
43
44
45
46
47
48
49
50
51
52
53
54
55
56
57
58
59
60
61
62
63
64
65

INTRODUCTION

In eukaryotic genomes, DNA is wrapped around octamers of histone proteins and the resulting nucleosomes are further folded into higher order chromatin structures. The state of chromatin packaging is controlled during growth and development and can regulate the temporal and spatial expression of genes (Jarillo et al. 2009; Pfluger and Wagner 2007; Reyes 2006). One mode of control is through the covalent modification of histone proteins by the addition of acetyl groups, usually at the histone's N-terminal domain (Chen and Tian 2007). Histone acetylation is controlled by transcriptional coactivator complexes including a histone acetyltransferase (HAT). The well-characterized histone acetyltransferase GCN5 physically interacts with the transcriptional adaptor protein ADA2; the essential nature of their interaction is indicated by the lack of acetylation when ADA2 is absent (Candau et al. 1997). In metazoans, it has been shown that GCN5 and ADA2b are both members of SAGA and SAGA-like (SLIK, STAGA) complexes and there is also evidence for the presence of GCN5 in a separable ATAC complex (Spedale et al. 2012). While biochemical or structural evidence has not been used to define these transcriptional coactivator complexes in plants, a SAGA complex(es) in which both GCN5 and ADA2b would function together has been predicted (Srivastava et al. 2015). Our previous work suggests that GCN5 and ADA2b also play separable roles and that the paralog ADA2a has minor phenotypic impact in *Arabidopsis* (Hark et al. 2009; Vlachonasios et al. 2003).

Both the *GCN5* and *ADA2* genes play a critical role in regulating metazoan growth and development. In *Drosophila*, loss of *GCN5* results in defects in oogenesis and metamorphosis (Carré et al. 2005), while in *Mus musculus*, disruption of *GCN5* leads to embryonic lethality (Xu et al. 2000; Yamauchi et al. 2000). In *Arabidopsis*, disruption of the *GCN5* and *ADA2b* genes affects the development and growth of stems, roots, and leaves (Bertrand et al. 2003; Vlachonasios et al. 2003). Specifically, T-DNA insertional mutations in *GCN5* (also known as *HAG1*; Pandey et al. 2002; Table 1) result in dwarfism, folded and serrated leaves, loss of apical dominance, and flower abnormalities underlying reduced fertility (Bertrand et al. 2003; Cohen et al. 2009; Vlachonasios et al. 2003). *ADA2b* (also known as *PROPORZI*) disruption alleles have also been described in the literature as exhibiting a similar overall phenotype including dwarfism, altered leaf morphology, and floral defects (Sieberer et al. 2003; Vlachonasios et al. 2003).

While it was previously noted that the *gcn5-1* and *ada2b-1* rosette leaves were modified in morphology and had smaller palisade mesophyll cells (Vlachonasios et al. 2003), effects on trichomes, the single-celled hairs, have not been previously described. Trichomes are an attractive developmental model, with their accessibility on the leaf surface and the well-characterized genetics underlying their development. A trichome originates from specification of an epidermal cell on rosette and cauline leaves, the stem, and even the flower's sepals in *Arabidopsis* (Hülkamp et al. 1994). Post-specification, four key processes (endoreduplication, branch formation, directional growth by cell expansion, and differentiation) contribute to morphogenesis. Specifically, three rounds of karyokinesis occur prior to increased cell size and stalk elongation. The incipient pair of branches mark

the primary branch point and appear just as the stalk begins to elongate. Further increase in cell size takes place after the fourth endoreduplication event and this is followed by secondary branching off the distal pointing branch and final differentiation of a mature 3-branched trichome (Hülkamp 2004; Hülkamp et al. 1994; Schellmann and Hülkamp 2005)

There is a considerable amount of literature describing genes involved in various stages of trichome development, including cell fate determination (patterning) and morphogenesis. The activator-inhibitor, lateral inhibition model for the genetic control of trichome patterning requires positive and negative regulators, most of which are initially expressed in all cells during leaf growth and expansion (Hülkamp 2004). *GLABRA3* (*GL3*; Payne et al. 2000) acts as part of a trimer of positive regulators and triggers the transcription of negative regulators, including *TRIPTYCHON* (*TRY*) (Schellmann et al. 2002; Schnittger et al. 1999). These inhibitors translocate to adjacent cells and make the activator complex nonfunctional, leading to a non-trichome fate. In the cells destined to become trichomes, the activator complex turns on the *GLABRA2* (*GL2*) and *SIAMESE* (*SIM*) genes among others (Bramsiepe et al. 2010; Grebe 2012; Morohashi and Grotewold 2009). The former initiates the pathway towards trichome differentiation (Rerie et al. 1994), while the latter triggers endoreduplication by inhibiting *CDKA* and *CYCD* (Churchman et al. 2006).

Endoreduplication, the process in which cells duplicate their DNA but do not undergo mitosis, is seen in many eukaryotes but is most common in plants. There is significant evidence that plant endoreduplication correlates with an increase in cell size (Breuer et al. 2007). For example, constitutively active *CDKA*;1 kinase leads to significantly reduced levels of endoreduplication, trichome size, and number of trichome branches (Dissmeyer et al. 2009). Other factors outside the cyclin/CDK family have also been shown to impact endoreduplication as well as trichome patterning and morphogenesis. *TRY* encodes for a MYB transcription factor that is known to impact both pattern formation of trichomes on the leaf and trichome branching (Hülkamp et al. 1994; Pesch and Hülkamp 2011; Schellmann et al. 2007). As noted above, *TRY* normally appears to act through a repression pathway, blocking endoreduplication and additional branching (Hülkamp et al. 1994; Schellmann et al. 2002). *KAKTUS* (*KAK*) encodes an E3 ubiquitin ligase (HECT protein) and loss of function results in increased trichome branching as well as enhanced endoreduplication events in trichomes (El Refy et al. 2004; Hülkamp et al. 1994). There are also other genes implicated in trichome differentiation that may have a less direct role in cell cycle control. For example, *ZWICHEL* (*ZWI*) encodes a member of the kinesin superfamily of motor proteins that binds to microtubules in a calmodulin-dependent manner. *ZWI* is involved in cell expansion/growth of the trichome stalk and, indirectly, in secondary branching, thus all *zwi* mutants have very short stalks and only primary branches (Oppenheimer et al. 1997).

Given the extensive study of trichomes as a model for cell differentiation, it is striking that the role of epigenetic factors in rosette leaf and especially trichome development has been

largely unreported. To determine how specific chromatin modifiers, GCN5 and ADA2b, function in concert with other transcriptional regulators to execute these developmental pathways, we used multiple approaches to identify the cellular and morphological defects of leaves and trichomes in the *gcn5* and *ada2b* mutants. We show that while disruption of either of these transcriptional coactivators leads to a reduction in the size of leaf mesophyll and pavement cells, *ada2b* mutants have reduced cell number and disruption of GCN5 tends to increase the number of cells in the mesophyll. *gcn5* and *ada2b* mutants also display differences in trichome branching and have opposite effects on endoreduplication. Taken together, our data supports the idea that these chromatin modifiers are required for the established relationship between ploidy levels with cell size and trichome branching. This work also contributes to the larger picture of how individual chromatin factors impact specific developmental pathways.

MATERIALS and METHODS

Plant growth and genotypes

Plants were germinated in soil and grown at 20-25°C under continuous light conditions. Plants were watered twice a week with half-strength Hoagland's solution. Unless otherwise noted, data was obtained from the first five true leaves (not cotyledons) between 3-5 weeks of age. Ws-2, Col-0, and Ler were used as wild type comparisons as appropriate. *ada2b-1* and *gcn5-1* (Vlachonasios et al. 2003) are T-DNA disruption alleles isolated from the University of Wisconsin (Madison, WI, USA) collection. *gcn5-5* (SALK_048427) and *hag1-6/gcn5-6* (SALK_150784) are from the Salk Institute collection (La Jolla, CA, USA); *gcn5-6* seeds were kindly provided by Jeff Long. *zwiA* (SALK_031704) seeds were graciously provided by Henrik Buschmann (uni-osnabrueck.de). Seeds harboring mutations in *TRIPTYCHON* (*try-EM1*; (Hülkamp et al. 1994) and *KAKTUS* (*kak1*; Perazza et al. 1999) were kindly donated by Martin Hülkamp.

The effects of three recessive *gcn5* T-DNA insertion alleles in different ecotype backgrounds were examined (Table 1). *gcn5-1* (Ws-2 ecotype) is a loss-of-function mutation, arising from a 3' T-DNA insertion disrupting sequence encoding the bromodomain (Vlachonasios et al. 2003; Benhamed et al. 2008), which binds acetyl-lysine residues and has been shown to play a critical role in GCN5's acetylation of nucleosomes in other species (Li et al. 2009; Cieniewicz et al. 2014). *gcn5-5* is a weak loss-of-function allele created by a T-DNA insertion in intron 10 in the Col-0 background (Cohen et al. 2009). *gcn5-6* in the Col-0 ecotype is most likely the strongest disruption allele, with a T-DNA insertion at the beginning of intron 1. *ada2b-1* results from T-DNA insertions in the middle of the *ADA2b* coding sequence (Vlachonasios et al. 2003).

Leaf analysis

Differential interference contrast (DIC) microscopy

Leaves were harvested and fixed immediately in ethanol: glacial acetic acid (3:1) for 12 hours at 4 °C. After fixation, leaves were dehydrated in a series of ethanol (30%, 50%,

70%, 80% and 100%) for 20 min each. Subsequently, the leaves were immersed in the clearing solution, chloral hydrate: glycerol: H₂O (8:2:1). Samples remained in the clearing solution for at least 12 hours at 4°C. The proximal and distal part of the leaf was removed and the lamina was dissected out along the mid vein. The two parts of the lamina were mounted onto a glass slide with *ca* 100 µl of the clearing solution, covered with coverslip (No 1) and sealed with ENTELLAN® (Merck, UK).

Imaging and data extraction

Slides were observed with a Nikon MicroPhot-SA microscope using DIC optics and images were captured with a Nikon CoolPix 990 digital camera. For determining the density and size of the pavement cells, images were taken at approximately half distance along the proximodistal and mediolateral axes. On average, 4 images per leaf were taken, *i.e.* 2 consecutive images per lamina side. Images of the mesophyll layer (palisade cells) were taken by focusing along the z-axis. The images were converted to TIFF files and imported into Image J 1.3' v software for further analysis. For cell size measurements, the scale was set according to a 100 µm scale that was photographed under the same conditions as the rest of the slides. Subsequently, the cell circumference was traced with the Image J tracing tool application and the cell area and perimeter were calculated. Cell density was determined by counting all the cells included in a fixed image area. Four images were taken per leaf and five leaves, each from a different plant, were used for each genotype. Cell density (number of cells per unit area) was calculated. Total leaf area was also calculated. Leaves were scanned on a flatbed scanner (HP Scanjet 8200) at 300dpi resolution. A ruler was also scanned for scale reference. The images were transferred into ImageJ in order to calculate area, perimeter, width and length of individual leaves using the "analyse particles" function. Images were processed using the Adobe Photoshop 7.0 package. The total number of cells within a cell layer of a whole leaf was then determined. Statistical significance was assessed using a T-test.

Flow cytometry (FCM)

Sample preparation: Nuclei extraction and DAPI staining

The amount of tissue used for FCM varied depending on the type and age of the tissue and the type of analysis. For determining the endopolyploidy level, whole leaf tissue was taken from 3 plants (only the 5th leaf of true leaves) at 15 days old. The tissue was placed in a petri dish, chopped finely with a razor blade in 500 µl of extraction buffer (Partec, Germany) and filtered through a 30 µm mesh (Partec). At this stage, the sample was either analyzed soon after preparation or it was frozen in liquid N₂ and stored at -70°C. Prior to analysis, frozen samples were left to thaw at room temperature and then 1 ml Cystain UV staining solution (Partec) was added.

Endopolyploidy analysis: Instrument setting and analysis

Endopolyploidy analysis was performed with a PAS II Ploidy analyzer (Partec, Germany) using an arc-lamp. The instrument was calibrated using 3 µm calibration beads (Ex: 488 nm, Partec, Germany) for the alignment of the argon ion laser and using trout erythrocytes for the arc-lamp (excitation for UV < 420 nm). Coefficients of variation (CV values) of

<4.0 for the calibration beads (main peaks for both FCS and SSC) and <2.0 for the trout erythrocytes were considered satisfactory for analysis. 20,000 events were counted in each run at an average speed of 50 events / sec. The CV value for most of the peaks obtained was <4, subject to the type and age of the tissue. The left cut-off point was set at 150 and the right cut-off at 999.9. All the data was acquired on a logarithmic amplification (Log3) scale unless otherwise stated. Endoreduplication index (EI) was calculated as described before (Barow and Meister 2002; Gegas et al. 2014).

Data analysis: Data extraction and statistics

The number of counts of each peak was obtained by manual gating. The mean number of counts for each peak and the standard deviation was calculated and their significance was tested by performing a Student's t-test (t-test).

Trichome analysis

Trichome dimensions

For experiments in the Ws-2 background, trichomes were isolated from first and second pair of leaves based on protocol by Zhang and Oppenheimer (2004). The leaves were incubated in 10:1 ethanol:acetic acid for 2 hours followed by three washes with PBST. Leaves were then placed under air vacuum for 15 minutes and incubated at 50°C for 3-4 hours. The trichomes were removed with a paintbrush and put into an Eppendorf tube. Prior to microscopy the trichomes were washed three times with PBST and glycerol was added. Photographs were taken and analyzed with Image J. Statistical analysis of the results were made using t-test.

Analysis of Col and *gcn5-6* used a protocol adapted from Marks et al. (2008). Rosette leaves (first through fifth) were placed in a centrifuge tube with 50 mgs RiboPure Zirconia beads (Ambion; 50 mgs/ 1 gram of leaves) and a solution (15 ml/1 gram of leaves) containing 50 mM EGTA and 1X PBS. The trichomes were dislodged from the leaves by vortexing the tube for 30 seconds and then keeping on ice for 30 seconds, for sixteen cycles. The material was poured through two layers of screen door mesh (Lowes). The trapped material was washed off the mesh with PBS and then poured through a 100µm sieve to capture the trichomes. The fluid that passed through the screen door mesh was also passed over the sieve. Trichomes trapped in the sieve were rinsed off with 1X PBS and stored in a tube at 7°C. Small samples of trichomes in PBS were placed on microscope slides and covered with clay-footed cover slips. The clay was depressed until the trichomes were flattened and then the coverslip edges were sealed with nail polish to prevent dehydration. Undamaged trichomes were photographed at 40X with a Motic camera attached to a Nikon Eclipse microscope. Motic Images Plus 2.0 ML software was used to measure trichome stem and branch length; stem length was defined as the distance from the base to the center of the trichome, while branch length was from the tip of the longest trichome branch to the center of the trichome. The t-test was used to compare the stem, branch, and total lengths (stem + branch lengths) between different genotypes.

Trichome branching

Rosette leaves (second and third, from four to five-week-old plants) were fixed in 3% glutaraldehyde with 0.1 M phosphate buffer (pH 6.8), and followed by fixation in 1% OsO₄ with 0.1 M phosphate buffer. After processing through ethanol dehydration series, the leaves were critically point dried with liquid carbon dioxide. Carbon adhesive (CCC by EMS) held the leaves to the stubs, which were then sputter coated with gold. Samples were examined at 15 kV with the ABT-60 scanning electron microscope.

Double mutants

The *gcn5-1; ada2b-1* double mutant was created using pollen from *gcn5-1* to fertilize *ada2b-1* heterozygous plants, since homozygous *ada2b-1* mutants display flower infertility. The resulting F1 generation was self-fertilized and the segregating F2 population was genotyped using KAPA2GTM Fast PCR (Kapa Biosystems) with the primers listed in Online Resource 1. Progeny that were homozygous for mutant alleles at both loci were identified by PCR.

The *gcn5-1; try-EM1* and *gcn5-1; zwiA* double mutants were created using pollen from *gcn5-1* to fertilize *try* or *zwi* mutants. The progeny were then backcrossed to Ler and Col-0 backgrounds respectively for at least four generations. The F2 population was evaluated for *try* mutant phenotype and genotyped for *zwiA* and *gcn5-1* mutations by PCR with gene and T-DNA specific primers.

Gene expression analysis

Leaf tissue was isolated at ~4 weeks post planting and flash frozen in liquid nitrogen. Tissue was ground under liquid nitrogen and RNA prepared using a RNeasy Plant Mini Kit (Qiagen). RNA concentrations were determined using a Nanodrop and between 0.5-1 µg RNA was used in cDNA reactions with High Capacity RNA to cDNA Kit (Applied Biosystems) or Maxima First Strand cDNA synthesis (Thermo Scientific). qPCR was carried out using a comparative Ct approach on an Applied Biosystems StepOne Plus instrument. Reactions were set up using the FAST Universal Master Mix 2X protocol (Applied Biosystems). TaqMan assays (Applied Biosystems) used include GCN5 (At0228249_g1), ZWI (At02187047_g1), TRY (At02321066_g1), KAK (At02170143_g1), and ACT8 (At02270958_gH). Three replicates were performed for each data point per experiment (biological replicates), with allowable standard deviations of Ct < 5%. RQ or fold change values for each experiment were log₂ transformed and averaged for each experimental condition. Semi-quantitative RT-PCR was conducted using various primers (Online Resource 1) directed at portions of the GCN5 cDNA and at a housekeeping gene (At4g26410).

RESULTS

Transcriptional coactivators are required for correct specification of leaf cell number and size

Development of lateral organs such as leaves involves spatially and temporally controlled changes in cell proliferation, growth, and differentiation that are mediated in part by

alterations in chromatin structure (Bertrand et al. 2003; Kalve et al. 2014; Servet et al. 2010; Vlachonasios et al. 2003). GCN5 and ADA2b play an essential role in leaf development and have been implicated in specifying correct cell size in mesophyll tissue (Vlachonasios et al. 2003). A more detailed microscopic analysis allowed us to extend these findings and assess possible effects on cell number. The *gcn5-1* mutant displayed smaller mesophyll and pavement cell size, but there was no significant difference between cell number in *gcn5-1* and Ws-2 leaves (Fig. 1a, b). Plants homozygous for the *GCN5* hypomorphic allele *gcn5-5* displayed increased cell number in the mesophyll but still showed reduced cell size (Fig. 1a, b). Loss of ADA2b resulted in a decreased number of mesophyll and pavement cells per leaf as well as reduced leaf cell size, resulting in smaller leaf area (Fig. 1a, b, c). Double mutant plants with disruption of both *GCN5* and *ADA2b* show some reduction in leaf area but not to the degree seen in *ada2b-1* single mutants (Fig. 1c).

GCN5 and ADA2b have opposite effects on ploidy

Because final cell size is often correlated with the number of rounds of endoreduplication (Gegas et al. 2014; Sugimoto-Shirasu and Roberts 2003; Traas et al. 1998), we investigated ploidy levels using flow cytometry analysis. We found that 50% of nuclei isolated from the fifth rosette leaf of 15-days old Ws-2 seedlings give rise to 2C or 4C peaks (Fig. 2a), suggesting that the bulk of this population of cells do not enter the endocycle (4C nuclei can represent mitotic cells in G2 or cells that have endocycled once). Ws-2 leaves also possess approximately 10% of 16C and 32C peaks. Nuclear content profiles for *gcn5-1* and *gcn5-5* were similar to wild type controls (Fig. 2a). *gcn5-6* displayed a higher proportion of 4C nuclei than wild type plants and a lower proportion of 16C and 32C nuclei (Fig. 2b). In contrast, *ada2b-1* plants displayed a reduced proportion of 2C and 4C peaks and notably higher 16C and 32C peaks (Fig. 2a). Nuclei counts were also used to calculate the Endoreduplication Index values (Barow and Meister 2003; Online Resource 2).

To extend these findings, we analyzed the ploidy levels in the *ada2b-1; gcn5-1* double mutant. The double mutant plant is dwarf (smaller than *gcn5-1*) and has characteristics of both *gcn5-1* and *ada2b-1* (Fig. 3a; Online Resource 3). In this experiment, the wild type plants showed slightly higher overall ploidy levels although the percentage of cells with less than 8C was similar between Ws-2 and *gcn5-1*, as shown in Fig. 2. The double mutant, however, shows reduced ploidy levels (Fig. 3b; Online Resource 2), indicative of fewer endocycles as compared to wild type plants.

Transcriptional coactivators impact trichome branch number, pattern, and expansion

Trichomes provide a readily accessible single cell system in which the role of chromatin modifiers in defining cell shape and size can be investigated. Development of *Arabidopsis* trichomes has been described in a series of stages (Mathur 2006; Szymanski et al. 1998, 2000) involving initially a radial expansion of the committed epidermal cell and then a vertical expansion, initiating the formation of the stalk. At the primary branch point, two branches arise and, after an increase in cell size, secondary branching takes place off the

distal branching point (Folkers et al. 1997; Szymanski et al. 1999). Changes in trichome branching were observed in plants harboring disruptions in *ADA2b* and *GCN5*. There were significant differences in the branch number of trichomes in *ada2b-1* plants, with an increase in unbranched and 2-branched trichomes and a decrease in 3-branched trichomes compared to wild type plants (Fig. 4a, b, g). A similar effect with another hypomorphic *ada2b* allele (*prz1-1*) was noted by Sieberer et al. (2003). A decrease in trichome branch number was also seen in *gcn5-1* mutants (Fig. 4c, h) and a trend towards decreasing branch number was observed in the *gcn5-5* background (Online Resource 4). Interestingly, plants homozygous for the likely null allele, *gcn5-6*, showed a significantly increased number of 4- (or more) branched trichomes (Fig. 4d, e, f). Comparison of 4-branched trichomes of Col-0 vs. *gcn5-6* plants uncovers a difference in patterning: *gcn5-6* predominantly has two primary branches that each undergo a secondary branching event while in Col, the most common pattern is one secondary branch undergoing an additional bifurcation (Fig. 5).

To examine whether *GCN5* and *ADA2b* affect the overall outgrowth of the trichome from the leaf surface, we measured the length of the trichome stem (stalk) as well as total trichome length. Both parameters were longer in *gcn5-1* and *ada2b-1* mutants than in wild type controls (Fig. 6a, b). In the *gcn5-6* background, the dimensions of 3- and 4-branched trichomes were examined separately. Three-branched *gcn5-6* trichomes had a statistically significant longer branch length than that of wild type trichomes and therefore a longer total trichome length (Fig. 6c). In 4-branched trichomes, *gcn5-6* mutants have a statistically shorter stem length (and shorter overall length) than that of Col-0 4-branched trichomes (Fig. 6d). There were no significant differences in the trichome area and perimeter in *gcn5-1* and *ada2b-1* plants in comparison with wild type controls (Online Resource 5). However, *gcn5-5* trichome area and perimeter were significantly smaller than the wild type plants (Online Resource 5).

GCN5 may define an additional circuit in the trichome developmental pathway

As our knowledge of details effects of chromatin modifiers increases, it will be interesting to understand how these factors act and interact with other cellular regulators to effect development. To test whether the histone acetyltransferase *GCN5* genetically interacts with known regulators of trichome branching, we examined the phenotypes of two double mutants, created by crossing *gcn5-1* plants with mutants of *ZWICHEL* (*ZWI*), which is a positive regulator of trichome branching, and the negative regulator *TRIPTYCHON* (*TRY*). *gcn5-1; zwia* plants primarily displayed unbranched trichomes, a more severe phenotype than either single mutant (Figure 7 and 4h). Two branched trichomes seen in *gcn5-1; zwia* double mutants displayed an underdeveloped, short second branch with a blunt tip, rather than an extended branch (Figure 7c). Trichomes of the *gcn5-1; zwia* double mutant also showed a swollen base, as in seen with *zwi* mutants in the Ws-2 background (Oppenheimer et al. 1997), and a very shortened trichome stalk characteristic of *zwi* mutants (Figure 7b, c). The double mutant plants display other characteristics of the overall *gcn5* mutant phenotype, e.g. dwarfism, leaf morphology differences (data not shown). *gcn5-1; try-EM1* double mutants displayed a degree of trichome branching that is similar to wild type controls (Figure 8). The overall plant phenotype resembled those of *gcn5* single mutants

(Figure 8).

To study whether possible interactions impact gene transcription, we assessed the expression levels of *ZWI* and *TRY* as well as the negative regulator *KAKTUS* in *gcn5-1* and *gcn5-6* mutants. Previous microarray analysis had shown that there was no change in *ZWI* expression and a slight increase (less than 3-fold) in *KAK* expression in *gcn5-1* mutants (Vlachonasios et al. 2003). We used qRT-PCR to assay *TRY* expression in a *gcn5-1* background and documented an average 4-fold decrease in expression (Figure 9). However, analysis of these three candidate genes in the *gcn5-6* mutant background did not reveal any consistent significant changes in gene expression (Figure 9). In addition, we analyzed expression levels of *GCN5* in *zwi*, *try*, and *kak* mutants. *GCN5* expression was increased in some individual mutant samples while the level remained similar to wild type in other isolates (Figure 9).

DISCUSSION

Our work provides valuable insights into how the transcriptional coactivators GCN5 and ADA2b impact leaf development at the tissue and cellular level, contributing to our understanding of how chromatin modifiers contribute to specific developmental processes. First, analysis of rosette leaves suggests that ADA2b is involved in both cell division and cell size (Fig. 1). A reduced rate of cell division in *ada2b-1* plants would be expected to result in fewer number of cells and smaller organs (Vlachonasios et al. 2003). Indeed, several members of the *KIP RELATED PROTEIN* (*KRP*) family have been shown to be misexpressed in an *ada2b* mutant background, which might contribute to deregulated cell proliferation upon auxin treatment (Anzola et al. 2010). The *gcn5-1* mutant displayed a wild type rate of division but showed reduced cell expansion. A weak GCN5 mutant allele, *gcn5-5*, displayed increased cell number, suggesting that GCN5 could also have an effect on cell proliferation depending on the allele or the genetic background (Fig. 1).

Secondly, our data show that GCN5 plays a role in trichome branching and that ADA2b acts specifically to promote trichome branch initiation. *ada2b-1* and *gcn5-1* trichomes were underbranched while *gcn5-6* plants displayed increased numbers of trichomes with four or more branches (Fig. 4). *gcn5-1* and *gcn5-5* are hypomorphs in the Ws-2 and Col-0 backgrounds respectively while *gcn5-6* (in Col-0 background) results from a T-DNA insertion after the first exon. Semi-quantitative RT-PCR analysis indicates that the full-length transcript is disrupted in both the *gcn5-1* and *gcn5-6* backgrounds (Vlachonasios et al. 2003; Online Resource 6), although the site of disruption in *gcn5-1* impacts only the end of the bromodomain (which binds acetyl-lysine) while in *gcn5-6*, the disruption impacts the catalytic HAT domain. The differences in *gcn5* mutant phenotypes may be interpreted in light of the varying underlying molecular lesions and/or genetic backgrounds; we have previously documented different allelic effects on flower morphology (Cohen et al. 2009).

Our data also revealed a reciprocal relationship between trichome stem length and branch

number (Fig. 6). *ada2b-1* and *gcn5-1* trichomes with reduced branching have a longer stem and overall trichome length, while trichome area and perimeter remain unchanged. Conversely, 4-branched trichomes seen in the *gcn5-6* background have a shorter stem and overall length. These results support the idea that by later stages of trichome differentiation the overall size of the cell is determined, such that decreased branching results in an extended stem and increased branching imposes a shorter stem. There may also be temporal control. If the primary branch point is established later, the trichome stem may extend and the number of branches that can form would be limited. In contrast, earlier establishment of the primary branch may shorten the stem and facilitate additional branching.

It is interesting to consider the specific morphology of the *gcn5-6* 4-branched trichomes (Fig. 5). The shorter stem length here is reminiscent of *zwichel* mutants, which show a more pronounced version of this effect. The predominant pattern of one primary and two secondary branching events seems both regular and similar to that seen in another trichome overbranching mutant, *kak-1* (Perazza et al. 1999). These observations supported the hypothesis that the transcriptional coactivators work in concert with transcription factors and other known regulators of trichome development. TRIPTYCHON (TRY) acts to block trichome branching such that loss-of-function mutations show increased branch number (Hülkamp et al. 1994). *gcn5-1; try-EM1* plants show a degree of trichome branching similar to wild type, showing that the two mutations offset each other and that GCN5 and TRY operate in independent pathways (Figure 8). Our data also suggests that GCN5 works in a separate pathway from ZWICHEL in its effects on trichome morphogenesis (Figure 7). Expression analysis (Figure 9) also generally supports the idea that GCN5 acts in a parallel pathway(s) to these established transcriptional regulators as well as the ubiquitin ligase KAKTUS to impact trichome development.

Benhamed et al. (2008) took a genome wide approach to identifying GCN5 interacting partners, by assessing promoter occupancy of GCN5 via a ChIP-chip approach. Relevant to the genes explored here, they detected binding of GCN5 at the ZWI promoter in wild type *Arabidopsis* seedlings but not in a *gcn5-1* mutant line. However, we have previously shown that there is no change in expression of ZWI in *gcn5-1* plants (Vlachonasios et al. 2003), supporting Benhamed et al.'s findings that not all promoters bound by GCN5 show resulting transcriptional effects. While we see modest effects on TRY and KAK in *gcn5-1* (Fig. 9; Vlachonasios et al. 2003), there was no reported change in promoter binding or expression of TRY and KAK in the *gcn5-1* mutant background in Benhamed et al. 2008. We confirmed this lack of interaction in the stronger *gcn5-6* allele. There is no support for other known regulators of trichome branching (e.g., GLABRA3, STICHEL, ANGUSTIFOLIA) interacting with GCN5 or ADA2b (Benhamed et al. 2008; Vlachonasios et al. 2003). Neither our current work nor these genome wide studies investigate gene expression in trichome cells specifically, in part due to limitations of the mutant plants' leaf mass.

Endoreduplication in plant leaves has been shown to impact cell size and trichome

differentiation (Breuer et al. 2007; Bramsiepe et al. 2010). *ada2b-1* mutants display increased ploidy levels, suggesting an earlier transition to the endocycle and increased rounds of endoreduplication (Fig. 2). Leaves of *gcn5* mutants tend to have reduced ploidy (Fig. 2), indicating another distinct function between ADA2b and GCN5 (Vlachonasios et al. 2003). It may be worth noting that Kim et al. (2015) reported that *gcn5-6* plants show an overall delay in leaf development, which might impact ploidy (and less trichomes on the abaxial surface). ADA2b appears to act as a negative regulator of endoreduplication independent of GCN5, such that plants lacking ADA2b alone show increased ploidy. *ada2b-1* plants would be predicted to lack functional SAGA complex but retain other GCN5 functions. The ploidy analysis of *gcn5* single and double mutants (Fig. 3) suggests that GCN5 acts to promote endoreduplication and is epistatic to ADA2b functions. The double mutant phenotype also suggests that ADA2b acts as an enhancer of GCN5 function in endoreduplication.

As *ada2b-1* plants display increased ploidy but decreased cell size, loss of ADA2b uncouples the established correlation between ploidy and leaf cell size (Melaragno et al. 1993). Increased endoreduplication is often associated with increased morphological complexity in a cell-type specific manner (Bramsiepe et al. 2010; Sugimoto-Shirasu and Roberts 2003). It is notable that in *ada2b* mutant leaves both pavement and trichome cells show reduced complexity (cell differentiation and trichome branching). Taken together our results suggest that ADA2b impinges on the transition between cell proliferation and differentiation and/or that ADA2b may mediate an endoreduplication-dependent mechanism for cell morphogenesis.

gcn5 and *ada2b* mutants also disrupt the link between endoreduplication and trichome branching (Hülkamp et al. 1999). *ada2b-1* plants show increased ploidy and yet have decreased trichome branch points. The strong mutant allele *gcn5-6* displays reduced ploidy in leaves but increased branching of some trichomes. While there are examples of mutant lines in which trichome branching is impacted while ploidy remains unchanged (e.g., *STICHEL* as described by Ilgenfritz et al. 2003 and *BRANCHLESS TRICHOMES* as described by Kasili et al. 2011), in our study we see the *opposite* of the predicted effect, i.e. ploidy levels are changed but not in a way that correlates with the established effect of endoreduplication promoting increased branch number. We acknowledge that our ploidy analysis is not of trichome cells specifically; however, others have observed similar levels of DNA content in leaves analyzed by flow-cytometry and trichomes assessed by DAPI staining (Churchman et al. 2006; Hamdoun et al. 2016; Kasili et al. 2011; Li et al. 2012).

In summary, we demonstrate developmental impacts on rosette leaf cell division and growth and trichome morphogenesis by the histone acetyltransferase GCN5 and the transcriptional coactivator ADA2b. This work contributes to the ultimate goal of linking these chromatin modifiers to specific developmental pathways within cells and tissues, for which we still have a limited number of examples (Benhamed et al. 2006). It is also interesting to note that loss of these transcriptional coactivators uncouples established connections between endoreduplication and other developmental events in rosette leaves.

In particular, ADA2b is required to promote the positive correlations between ploidy and cell size as well as between rounds of endoreduplication and trichome branching. In general, our results support the overlapping and distinct developmental functions for these chromatin modifiers and highlight ADA2b's role as a cellular regulator beyond participation as a partner with GCN5.

AUTHOR CONTRIBUTION

Substantial contributions to the conception or design of the work (JK, JD, KV, EM, AH), data acquisition (JK, MSa, VG, NP, AK, PP, AM, MSh, JB, ALK, CK, GW, HC, KV, EM, AH), and/or interpretation of data (JK, VG, MSh, JB, ALK, CK, GW, HC, JD, KV, EM, AH) were made by all authors. Authors participated in drafting the work (JK, MSa, VG, NP, AK, PP, AM, MSh, JB, ALK, CK, GW, HC, JD, KV, EM, AH) and/or revising it critically for important intellectual content (JK, JD, KV, EM, AH). All authors have given final approval of the manuscript and agree to be accountable for all aspects of the work.

ACKNOWLEDGEMENTS

We thank Muhlenberg College students Max Blumenthal and Timothy DeRosa for contributions to the gene expression studies and acknowledge Hannah Molk for her preliminary work investigating the GCN5 transcript in *gcn5-6* plants. We also thank AUTH undergraduate students Dimitra Papadopoulou, Zoe Spyropoulou, Anthi Symeonidou and Dimitra Tsompani for contributions to genetic analysis of double mutants. Permission to adapt Fig. 5 from Folkers et al. (1997) was kindly granted by The Company of Biologists Ltd.

FUNDING

This work was supported in part by Muhlenberg College. A Gene and Development British Society summer studentship was granted to PN and Erasmus+ placement to PP and SM.

REFERENCES

- Alonso JM, Stepanova AN, Leisse TJ, Kim CJ, Chen H, Shinn P, et al (2003) Genome-wide insertional mutagenesis of *Arabidopsis thaliana*. *Science* 301: 653–657. doi:10.1126/science.1086391.
- Anzola JM, Sieberer T, Ortbauer M, Butt H, Korbei B, Weinhofer I, et al (2010) Putative *Arabidopsis* Transcriptional Adaptor Protein (PROPORZ1) is required to modulate histone acetylation in response to auxin. *Proc Natl Acad Sci* 107: 10308–10313. doi:10.1073/pnas.0913918107.
- Barow M and Meister A (2002) Lack of correlation between AT frequency and genome

size in higher plants and the effect of nonrandomness of base sequences on dye binding. *Cytometry* 47: 1–7.

Benhamed M, Bertrand C, Servet C, and Zhou D-X (2006) Arabidopsis GCN5, HD1, and TAF1/HAF2 interact to regulate histone acetylation required for light-responsive gene expression. *Plant Cell* 18: 2893–2903. doi:10.1105/tpc.106.043489.

Benhamed M, Martin-Magniette M-L, Taconnat L, Bitton F, Servet C, De Clercq R, et al (2008) Genome-scale Arabidopsis promoter array identifies targets of the histone acetyltransferase GCN5. *Plant J* 56: 493–504. doi:10.1111/j.1365-313X.2008.03606.x.

Bertrand C, Bergounioux C, Domenichini S, Delarue M, and Zhou D-X (2003) Arabidopsis histone acetyltransferase AtGCN5 regulates the floral meristem activity through the WUSCHEL/AGAMOUS pathway. *J Biol Chem* 278: 28246–28251. doi:10.1074/jbc.M302787200.

Bramsiepe J, Wester K, Weinl C, Roodbarkelari F, Kasili R, Larkin JC, et al (2010) Endoreplication controls cell fate maintenance. *PLoS Genet.* 6, e1000996. doi:10.1371/journal.pgen.1000996.

Breuer C, Stacey NJ, West CE, Zhao Y, Chory J, Tsukaya H, et al (2007) BIN4, a novel component of the plant DNA topoisomerase VI complex, is required for endoreduplication in Arabidopsis. *Plant Cell* 19: 3655–3668. doi:10.1105/tpc.107.054833.

Buschmann H, Dols J, Kopischke S, Peña EJ, Andrade-Navarro MA, Heinlein M, et al (2015) Arabidopsis KCBP interacts with AIR9 but stays in the cortical division zone throughout mitosis via its MyTH4-FERM domain. *J Cell Sci* 128: 2033–2046. doi:10.1242/jcs.156570.

Candau R, Zhou JX, Allis CD, and Berger SL (1997) Histone acetyltransferase activity and interaction with ADA2 are critical for GCN5 function in vivo. *EMBO J* 16: 555–565. doi:10.1093/emboj/16.3.555.

Carré C, Szymczak D, Pidoux J, and Antoniewski C (2005) The histone H3 acetylase dGcn5 is a key player in *Drosophila melanogaster* metamorphosis. *Mol Cell Biol* 25: 8228–8238. doi:10.1128/MCB.25.18.8228-8238.2005.

Chen ZJ and Tian L (2007) Roles of dynamic and reversible histone acetylation in plant development and polyploidy. *Biochim Biophys Acta* 1769: 295–307. doi:10.1016/j.bbaexp.2007.04.007.

Churchman ML, Brown ML, Kato N, Kirik V, Hülkamp M, Inzé D, et al (2006) SIAMESE, a plant-specific cell cycle regulator, controls endoreplication onset in Arabidopsis thaliana. *Plant Cell* 18: 3145–3157. doi:10.1105/tpc.106.044834.

Cieniewicz AM, Moreland L, Ringel AE, Mackintosh SG, Raman A, Gilbert TM, et al (2014) The bromodomain of Gcn5 regulates site specificity of lysine acetylation on histone H3. *Mol Cell Proteomics* 13: 2896-2910. doi: 10.1074/mcp.M114.038174.

Cohen R, Schocken J, Kaldis A, Vlachonasios KE, Hark AT, and McCain ER (2009) The histone acetyltransferase GCN5 affects the inflorescence meristem and stamen development in *Arabidopsis*. *Planta* 230: 1207–1221. doi:10.1007/s00425-009-1012-5.

Dissmeyer N, Weimer AK, Pusch S, De Schutter K, Alvim Kamei CL, Nowack MK, et al (2009) Control of cell proliferation, organ growth, and DNA damage response operate independently of dephosphorylation of the *Arabidopsis* Cdk1 homolog CDKA;1. *Plant Cell* 21: 3641–3654. doi:10.1105/tpc.109.070417.

El Refy A, Perazza D, Zekraoui L, Valay J-G, Bechtold N, Brown S, et al (2004) The *Arabidopsis* KAKTUS gene encodes a HECT protein and controls the number of endoreduplication cycles. *Mol Genet Genomics* 270: 403–414. doi:10.1007/s00438-003-0932-1.

Folkers U, Berger J, Hülskamp M (1997) Cell morphogenesis of trichomes in *Arabidopsis*: differential control of primary and secondary branching by branch initiation regulators and cell growth. *Development* 124: 3779–3786.

Gegas VC, Wargent JJ, Pesquet E, Granqvist E, Paul ND, Doonan JH (2014) Endopolyploidy as a potential alternative adaptive strategy for *Arabidopsis* leaf size variation in response to UV-B. *J Exp Bot* 65: 2757–2766. doi:10.1093/jxb/ert473.

Grebe M (2012) The patterning of epidermal hairs in *Arabidopsis* — updated. *Curr Opin Plant Biol* 15: 31–37. doi:10.1016/j.pbi.2011.10.010.

Hark AT, Vlachonasios KE, Pavangadkar KA, Rao S, Gordon H, Adamakis I-D, et al (2009) Two *Arabidopsis* orthologs of the transcriptional coactivator ADA2 have distinct biological functions. *Biochim Biophys Acta* 1789: 117–124. doi:10.1016/j.bbagr.2008.09.003.

Hülskamp M (2004) Plant trichomes: a model for cell differentiation. *Nat Rev Mol Cell Biol* 5: 471–480. doi:10.1038/nrm1404.

Hülskamp M, Misra S, Jürgens G (1994) Genetic dissection of trichome cell development in *Arabidopsis*. *Cell* 76: 555–566.

Hülskamp M, Schnittger A, Folkers U (1999) Pattern formation and cell differentiation: trichomes in *Arabidopsis* as a genetic model system. *Int Rev Cytol* 186: 147–178.

Ilgenfritz H, Bouyer D, Schnittger A, Mathur J, Kirik V, Schwab B, et al (2003) The Arabidopsis STICHEL gene is a regulator of trichome branch number and encodes a novel protein. *Plant Physiol* 131: 643–655. doi:10.1104/pp.014209.

Jarillo JA, Piñeiro M, Cubas P, Martínez-Zapater JM (2009) Chromatin remodeling in plant development. *Int J Dev Biol* 53: 1581–1596. doi:10.1387/ijdb.072460jj.

Kalve S, De Vos D, Beemster GTS (2014) Leaf development: a cellular perspective. *Front Plant Sci* 5: 362. doi:10.3389/fpls.2014.00362.

Kasili R, Huang CC, Walker JD, Simmons LA, Zhou J, Faulk C, et al (2011) BRANCHLESS TRICHOMES links cell shape and cell cycle control in Arabidopsis trichomes. *Development* 138: 2379–2388. doi:10.1242/dev.058982.

Kim J-Y, Oh JE, Noh Y-S, Noh B (2015) Epigenetic control of juvenile-to-adult phase transition by the Arabidopsis SAGA-like complex. *Plant J* 83: 537–545. doi:10.1111/tpj.12908.

Li S, Shogren-Knaak MA (2009) The Gcn5 bromodomain of the SAGA complex facilitates cooperative and cross-tail acetylation of nucleosomes. *J Biol Chem* 284:9411–9417. doi: 10.1074/jbc.M809617200.

Long JA, Ohno C, Smith ZR, Meyerowitz EM (2006). TOPLESS regulates apical embryonic fate in Arabidopsis. *Science* 312: 1520–1523. doi:10.1126/science.1123841.

Marks MD, Betancur L, Gilding E, Chen F, Bauer S, Wenger JP, et al (2008) A new method for isolating large quantities of Arabidopsis trichomes for transcriptome, cell wall and other types of analyses. *Plant J* 56:483–492. doi:10.1111/j.1365-313X.2008.03611.x.

Mathur J (2006) Trichome cell morphogenesis in Arabidopsis: a continuum of cellular decisions. *Can J Bot* 84: 604–612.

Melaragno JE, Mehrotra B, Coleman AW (1993) Relationship between Endopolyploidy and Cell Size in Epidermal Tissue of Arabidopsis. *Plant Cell* 5: 1661–1668. doi:10.1105/tpc.5.11.1661.

Morohashi K, Grotewold E (2009) A systems approach reveals regulatory circuitry for Arabidopsis trichome initiation by the GL3 and GL1 selectors. *PLoS Genet* 5, e1000396. doi:10.1371/journal.pgen.1000396.

Oppenheimer DG, Pollock MA, Vacik J, Szymanski DB, Ericson B, Feldmann K, et al (1997) Essential role of a kinesin-like protein in Arabidopsis trichome morphogenesis. *Proc Natl Acad Sci USA* 94: 6261–6266.

Pandey R, Müller A, Napoli CA, Selinger DA, Pikaard CS, Richards EJ, et al (2002) Analysis of histone acetyltransferase and histone deacetylase families of *Arabidopsis thaliana* suggests functional diversification of chromatin modification among multicellular eukaryotes. *Nucleic Acids Res* 30: 5036–5055.

Payne CT, Zhang F, Lloyd AM (2000) GL3 encodes a bHLH protein that regulates trichome development in *Arabidopsis* through interaction with GL1 and TTG1. *Genetics* 156: 1349–1362.

Perazza D, Herzog M, Hülskamp M, Brown S, Dorne AM, Bonneville JM (1999) Trichome cell growth in *Arabidopsis thaliana* can be derepressed by mutations in at least five genes. *Genetics* 152: 461–476.

Pfluger J, Wagner D (2007) Histone modifications and dynamic regulation of genome accessibility in plants. *Curr Opin Plant Biol* 10: 645–652. doi:10.1016/j.pbi.2007.07.013.

Rerie WG, Feldmann KA, Marks MD (1994) The GLABRA2 gene encodes a homeodomain protein required for normal trichome development in *Arabidopsis*. *Genes Dev* 8: 1388–1399.

Reyes JC (2006) Chromatin modifiers that control plant development. *Curr Opin Plant Biol* 9:21–27. doi:10.1016/j.pbi.2005.11.010.

Schellmann S, Hülskamp M (2005) Epidermal differentiation: trichomes in *Arabidopsis* as a model system. *Int J Dev Biol* 49: 579–584. doi:10.1387/ijdb.051983ss.

Schellmann S, Schnittger A, Kirik V, Wada T, Okada K, Beermann A, et al (2002). TRIPTYCHON and CAPRICE mediate lateral inhibition during trichome and root hair patterning in *Arabidopsis*. *EMBO J* 21: 5036–5046. doi:10.1093/emboj/cdf524.

Servet C, Conde E Silva N, Zhou, D-X (2010) Histone Acetyltransferase AtGCN5/HAG1 Is a Versatile Regulator of Developmental and Inducible Gene Expression in *Arabidopsis*. *Mol Plant* doi:10.1093/mp/ssq018.

Sieberer T, Hauser M-T, Seifert GJ, Luschig C (2003) PROPORZ1, a putative *Arabidopsis* transcriptional adaptor protein, mediates auxin and cytokinin signals in the control of cell proliferation. *Curr Biol* 13, 837–842.

Spedale G, Timmers HTM, Pijnappel WW (2012) ATAC-king the complexity of SAGA during evolution. *Genes Dev* 26: 527–541. doi:10.1101/gad.184705.111.

Srivastava R, Rai KM, Pandey B, Singh SP, Sawant SV (2015) Spt-Ada-Gcn5-Acetyltransferase (SAGA) Complex in Plants: Genome Wide Identification, Evolutionary

Conservation and Functional Determination. PloS One 10, e0134709.
doi:10.1371/journal.pone.0134709.

Sugimoto-Shirasu K, Roberts K (2003) “Big it up”: endoreduplication and cell-size control in plants. Curr Opin Plant Biol 6: 544–553.

Szymanski DB, Jilk RA, Pollock SM, Marks MD (1998) Control of GL2 expression in Arabidopsis leaves and trichomes. Development 125: 1161–1171.

Szymanski DB, Lloyd AM, Marks MD (2000) Progress in the molecular genetic analysis of trichome initiation and morphogenesis in Arabidopsis. Trends Plant Sci 5: 214–219.

Szymanski DB, Marks MD, Wick SM (1999) Organized F-actin is essential for normal trichome morphogenesis in Arabidopsis. Plant Cell 11: 2331–2347.

Traas J, Hülskamp M, Gendreau E, Höfte H (1998) Endoreduplication and development: rule without dividing? Curr Opin Plant Biol 1: 498–503.

Vlachonasios KE, Thomashow MF, Triezenberg SJ (2003) Disruption mutations of ADA2b and GCN5 transcriptional adaptor genes dramatically affect Arabidopsis growth, development, and gene expression. Plant Cell 15: 626–638.

Xu W, Edmondson DG, Evrard YA, Wakamiya M, Behringer RR, and Roth SY (2000) Loss of Gcn5l2 leads to increased apoptosis and mesodermal defects during mouse development. Nat. Genet 26: 229–232. doi:10.1038/79973.

Yamauchi T, Yamauchi J, Kuwata T, Tamura T, Yamashita T, Bae N, et al (2000) Distinct but overlapping roles of histone acetylase PCAF and of the closely related PCAF-B/GCN5 in mouse embryogenesis. Proc Natl Acad Sci USA 97: 11303–11306.
doi:10.1073/pnas.97.21.11303.

Zhang X, Oppenheimer DG (2004) A simple and efficient method for isolating trichomes for downstream analyses. Plant Cell Physiol 45: 221–224.

FIGURE CAPTIONS

Fig. 1 Analysis of (a) mean cell number per leaf, (b) mean cell area of mesophyll and pavement cells, and (c) mean leaf area in wild type (Ws-2 and Col-0) and mutant plants (n=5 leaves). A statistically significant difference between mutant lines and the relevant wildtype background is denoted p<0.001 with *** and p<=0.05 with *. Error bars represent standard error.

Fig. 2 Analysis of DNA content in wild type and mutant leaves. (a) The mean percent nuclei exhibiting specific ploidy levels in Ws-2 and Col-0 and the single mutants *gcn5-1*,

ada2b-1, and *gcn5-5* (n=3). Note that there were no ³²C nuclei detected in Ws, *gcn5-1*, or *gcn5-5* backgrounds. (b) The mean percent nuclei exhibiting specific levels of DNA content in Col-0 and *gcn5-6* (n=7) cells. Error bars represent standard error.

Fig. 3 Phenotype of the Ws-2, single mutants *ada2b-1* and *gcn5-1*, and the double mutant *ada2b-1; gcn5-1*. (a) Plant growth 30 and 57 days post planting. (b) DNA content analysis of Ws-2, double mutant and *gcn5-1* (n=3). Error bars represent standard error.

Fig. 4 Trichome branch arrangements and numbers on wild type and mutant leaves. Scanning electron micrographs illustrate predominant branching pattern for (a) 3-branched Ws, (b) 2-branched *ada2b-1*, (c) 2-branched *gcn5-1*, (d) 3-branched Col-0, (e) 4-branched *gcn5-6* and (f) 5-branched *gcn5-6*. Bar = 100 μ m. (g-i) The mean percentage of trichomes with 0 (unbranched), 2, 3, or 4+ branches. The number of trichomes having 0, 2, 3 or 4+ branches (x axis) is represented as a percentage of the total number of trichomes on a given second rosette leaf. Error bars represent standard error. (g) Comparison between *ada2b-1* leaves (n=32) and Ws-2 leaves (n=10). (h) Comparison between *gcn5-1* leaves (n=16) and Ws (n=19). (i) Comparison between *gcn5-6* leaves (n=16) and Col-0 (n=23). All branching categories in the mutants are significantly different from wildtype plants, with p values equal to or much less than < 0.05 . Error bars represent standard error.

Fig. 5 Trichome anatomy and the three most common 4-branch patterns observed in Col-0 and *gcn5-6*. (a) A typical 3-branched *Arabidopsis* trichome measured from a center point on the trichome; secondary branch (dashed line), primary branch (dotted line) and stem (solid line) are shown. Bar = 100 μ m. (b) The most common patterns for 4-branched trichomes (adapted with permission from Folkers et al., 1997. *Development*.124, 3781. <http://dev.biologists.org/content/124/19/3779.long>), which we refer to as types A, B, and C. Yellow circles denote primary branch point and blue circles denote secondary branch point. (c-e) Representative scanning electron microscope images of (c) type A, (d) type B, and (e) type C. Bar = 100 μ m. (f) The percent of surveyed Col-0 (n=43) and *gcn5-6* (n=43) trichomes from seven leaves that exhibit specific branching patterns.

Fig. 6 Measurements of trichome dimensions (μ m). (a) Mean trichome stem length. (b) Mean trichome total length. n=50 for all genotypes. (c) Mean stem, branch and total trichome length of 3-branched trichomes in Col-0 (n=171) and *gcn5-6* (n=169). (d) Mean stem, branch, and total trichome length of 4-branched trichomes in Col-0 (n=65) and *gcn5-6* (n=56). Statistical significance of the difference between wildtype and mutant plants is denoted with *p<0.1, **p<0.01, and ***p<0.001. Error bars represent standard error.

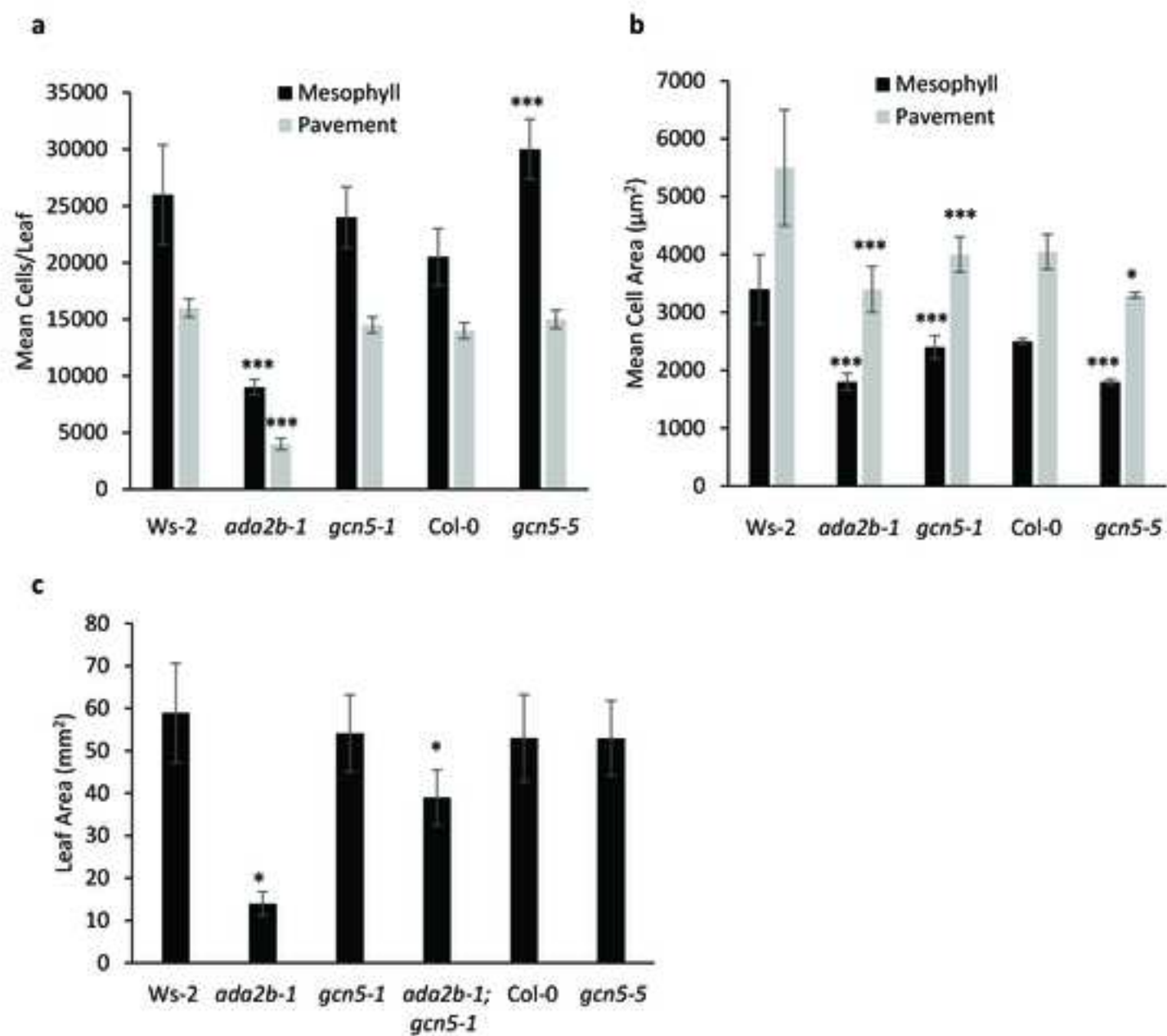
Fig. 7 *zwiA* single and *gcn5-1; zwiA* double mutants. (a) Light microscopy of double mutant. (b) Scanning electron microscopy of *zwiA* single mutant revealing the two types of 2-branched trichomes. Bar =100 μ m. (c) Scanning electron microscopy of *gcn5-1; zwiA* double mutant illustrating many trichomes with the strong *zwi* phenotype. Bar = 100 μ m. (d) Quantitative analysis of trichome branch number (compiled using SEM) in double mutants (n=12 leaves) and *zwiA* (n=17 leaves). The numbers of unbranched trichomes and

trichomes having 2 branches are represented as a percentage of the total number of trichomes on a given leaf. Error bars represent standard error; p values are $<<0.05$ for comparison of both unbranched and two-branched trichomes between the *zwiA* single mutant and the double mutant genotype. Col (n=8 leaves, 298 trichomes) displayed no unbranched trichomes and only two 2-branched trichomes.

Fig. 8 Analysis of Ler (a, d), the single mutants *try-EM1* (b, f), *gcn5-1* (c, e), and the double mutant *try-EM1; gcn5-1* (b, g). Plant growth 50 (a) or 40 (b, c) days after seed planting of genotypes as marked. (d-g) Gross leaf morphology and trichome distribution. (h) Branching patterns of each plant type were determined from eight to fourteen plants, 4 leaves per plant, and for a total of 108-148 trichomes.

Fig. 9 Gene expression changes as revealed by qRT-PCR. The average fold difference in expression is represented as its log₂ value, such that values between 1.0 and -1.0 indicate less than a 2-fold difference. Positive values indicate increased expression of the target gene in the mutant background. Error bars indicate standard deviation. n indicates the number of different plants (biological replicates) used.

Figure 1



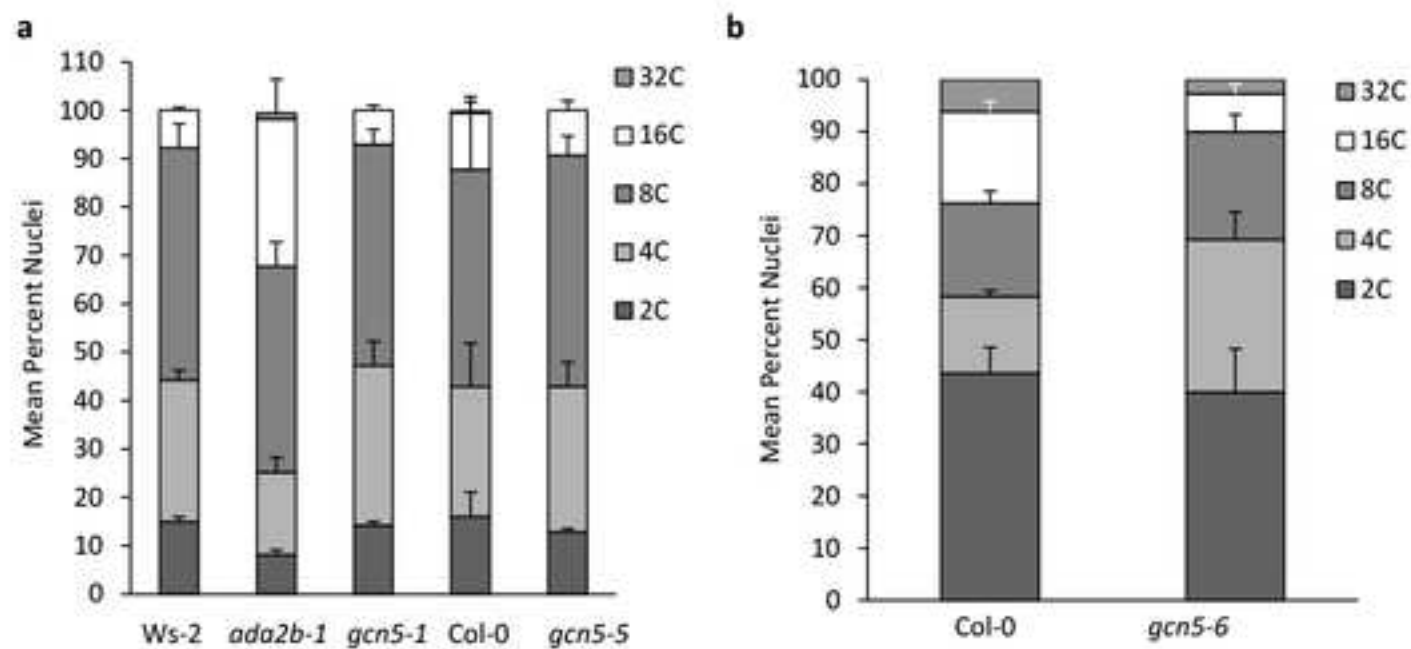


Figure 2

Figure 3

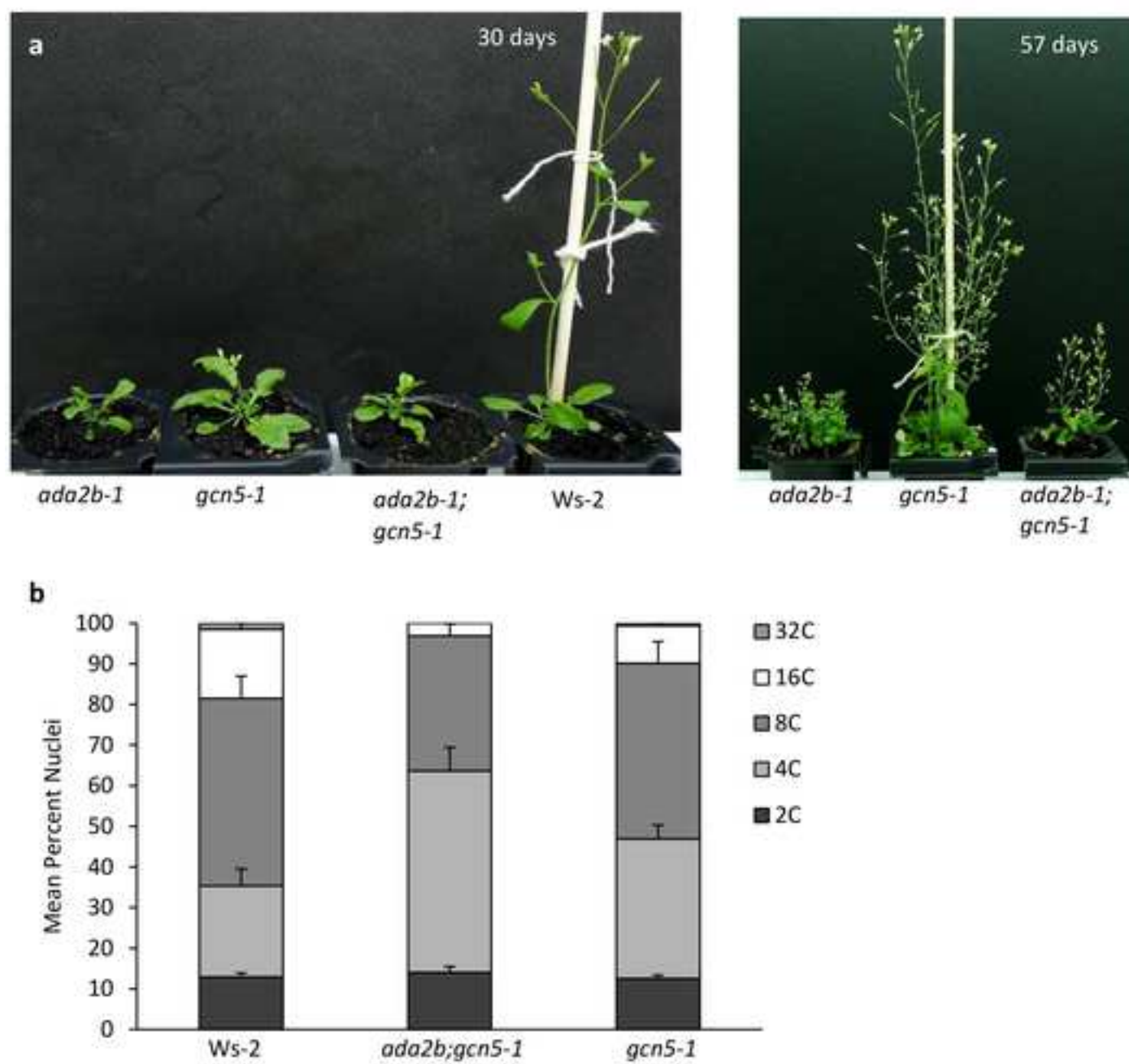
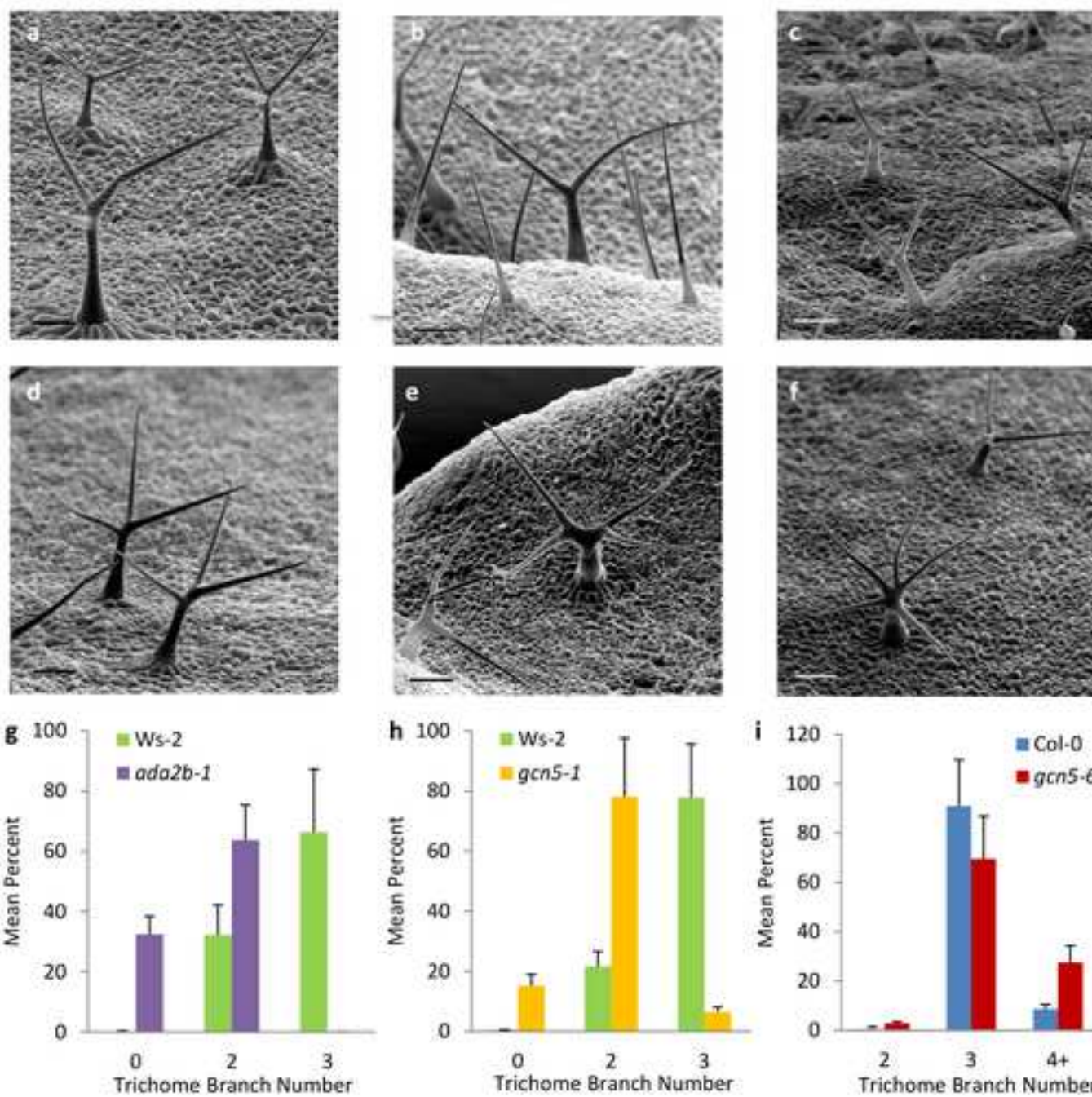


Figure 4



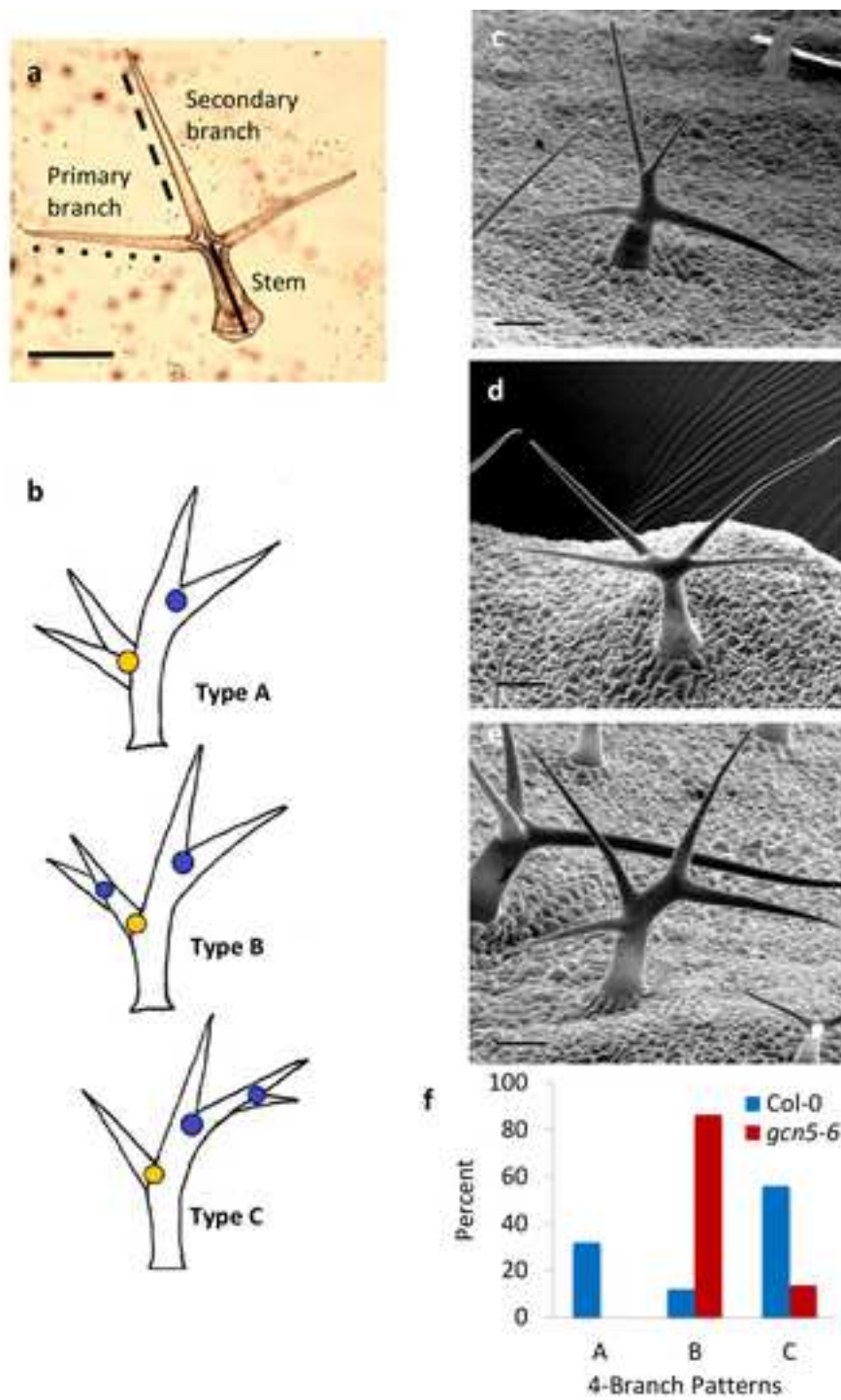


Figure 5

Figure 6

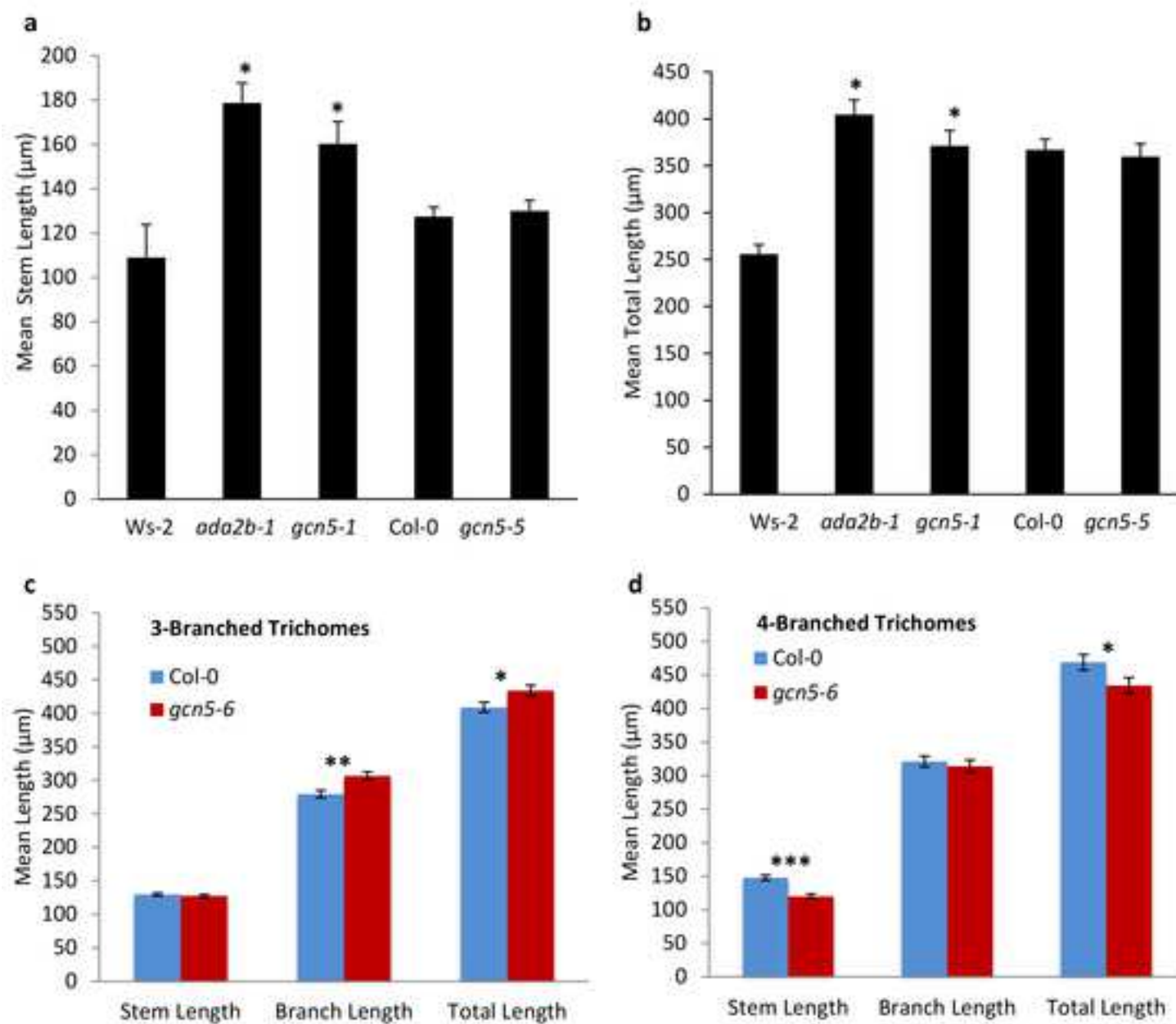
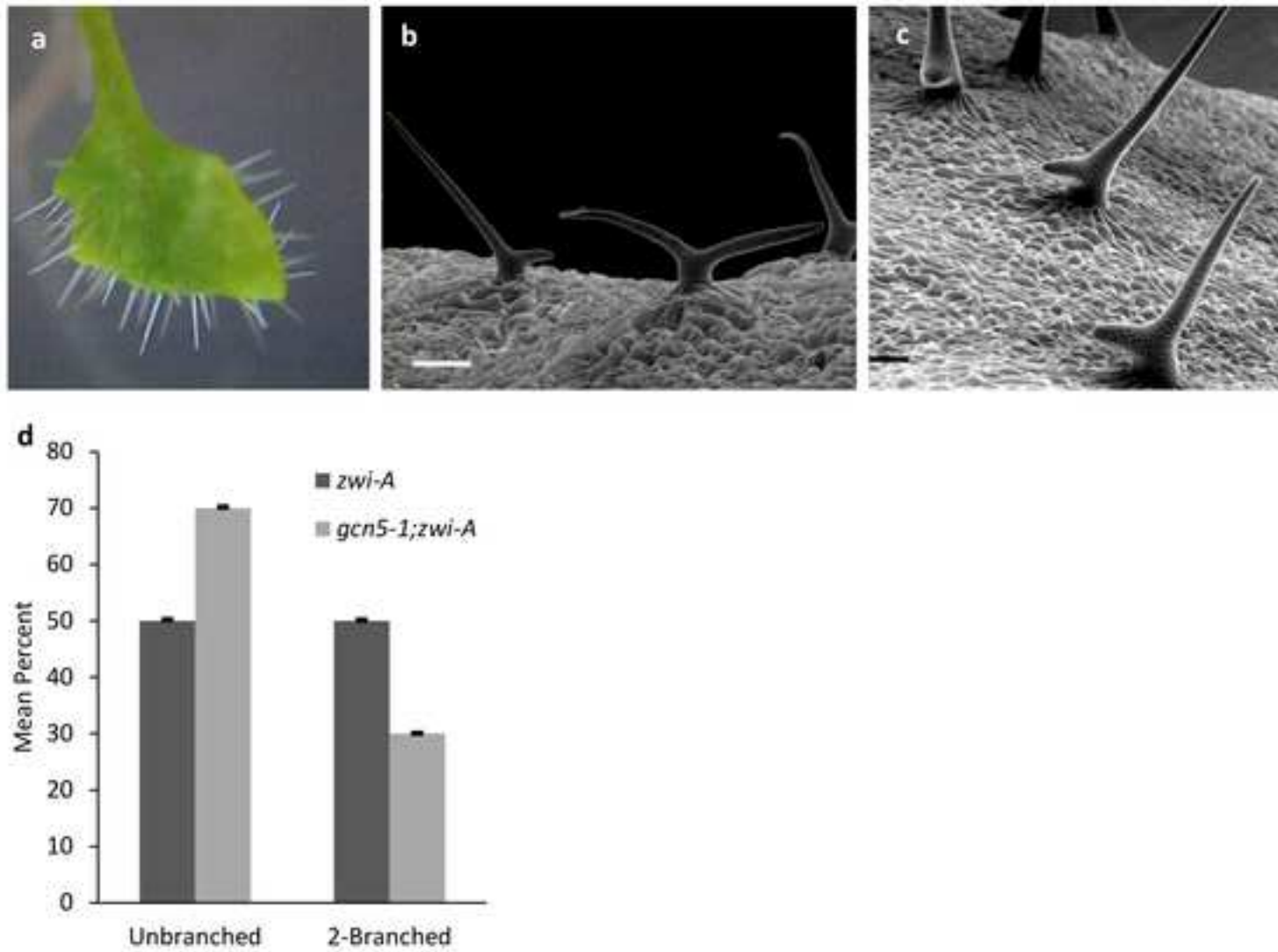


Figure 7



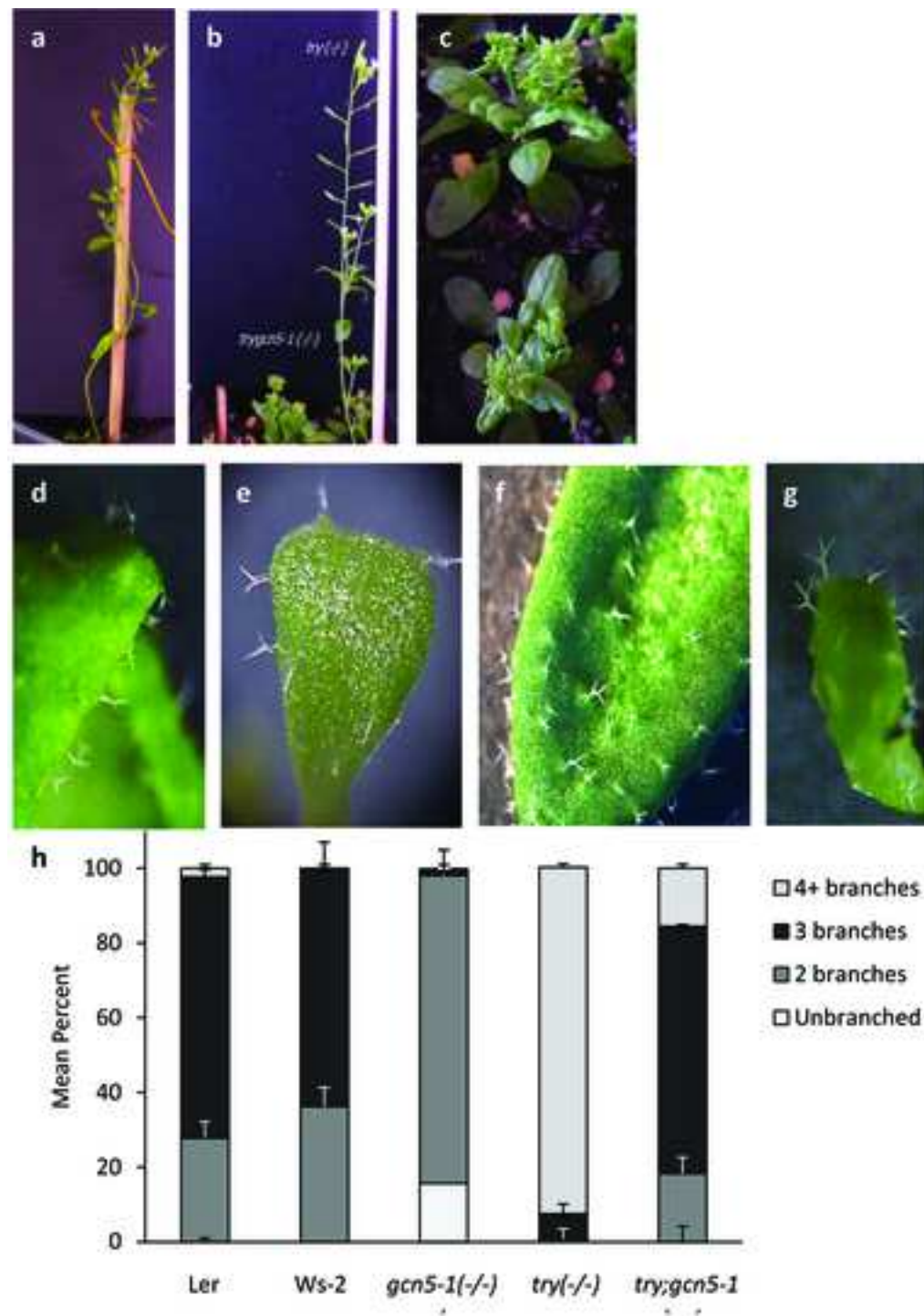


Figure 8

Figure 9

Target	ZWI	KAK	TRY	TRY	GCN5	GCN5	GCN5
Background	<i>gcn5-6</i>	<i>gcn5-6</i>	<i>gcn5-1</i>	<i>gcn5-6</i>	<i>zwi</i>	<i>kak</i>	<i>try</i>
(n)	4	3	5	4	5	3	5

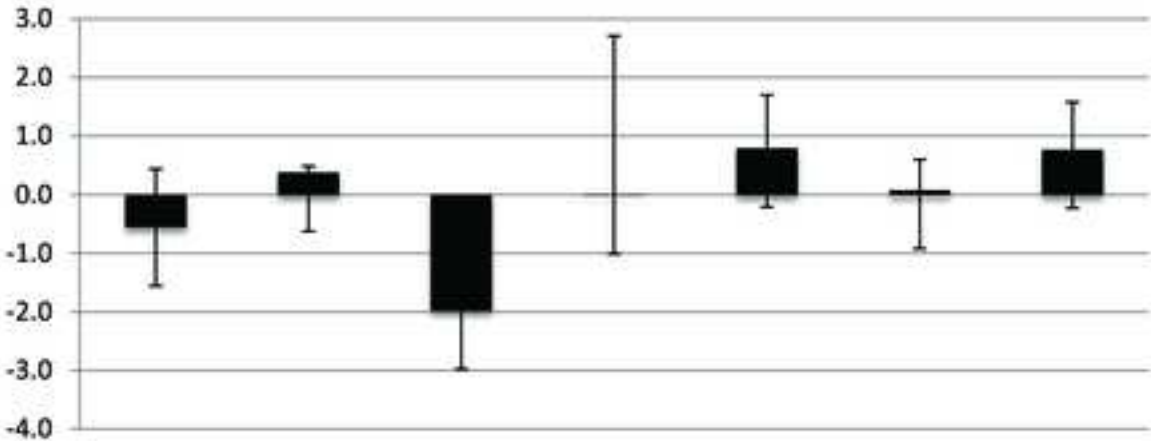
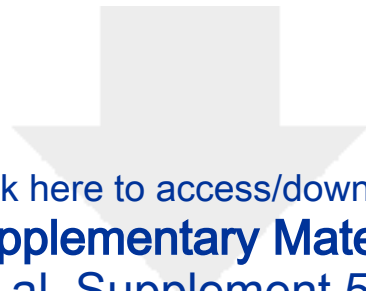


Table 1. Summary of mutant allelic backgrounds. References for trichome phenotypes of other *zwi* alleles are given in italics.

Mutant allele	Ecotype background	Type of mutation	Trichome phenotype	References
<i>gcn5-1</i>	Ws-2	T-DNA insertion in last exon, disrupts bromodomain	Reduced branching (present study)	Vlachonasios et al., 2003
<i>gcn5-5/hag1-5</i>	Col-0	T-DNA insertion in intron 10	Trend towards decreased branching (present study)	Long et al., 2006
<i>gcn5-6/hag1-6</i>	Col-0	T-DNA insertion at end of exon 1	Increased branching (present study)	Long et al., 2006
<i>ada2b-1</i>	Ws-2	T-DNA insertion in fifth intron, results in shortened, non-functional transcript	Reduced branching (present study)	Vlachonasios et al., 2003
<i>zwiA</i>	Col-0	T-DNA insertion in third exon	Reduced branching and shortened stalk (present study)	Alonso et al., 2003; Buschmann et al., 2015; <i>Hulskamp et al., 1994</i> ; <i>Oppenheimer et al., 1997</i>
<i>try-EM1</i>	Ler	EMS lesion	Increased branching and trichome clusters	Hulskamp et al., 1994
<i>kak-1</i>	Ler	EMS lesion	Increased branching	Hulskamp et al., 1994; Perazza et al., 1999



[Click here to access/download](#)

Supplementary Material

Kotak et al. Supplement 5.1.18.pdf